RSC Advances

RSC Publishing

COMMUNICATION

Flexible high performance wet-spun graphene fiber supercapacitors†

Cite this: *RSC Adv.*, 2013, **3**, 23957

Received 4th August 2013
Accepted 18th September 2013

DOI: 10.1039/c3ra44935a

www.rsc.org/advances

Tieqi Huang,[a] Bingna Zheng,[a] Liang Kou,[a] Karthikeyan Gopalsamy,[a] Zhen Xu,[a] Chao Gao,*[a] Yuena Meng[b] and Zhixiang Wei*[b]

We have explored a new method to produce flexible and all-solid-state graphene fiber supercapacitors (GFSs) from wet-spun graphene fibers. The GFSs exhibited high capacitance (3.3 mF cm^{-2}) and good stability (almost no changes occur after 5000 charge cycles and bending cycles). Moreover, we decorated GFSs with polyaniline nanoparticles and the resulting pseudocapacitors exhibited a capacitance of 66.6 mF cm^{-2}.

Introduction

Electrochemical capacitors (ECs), also known as supercapacitors, have shown their importance for energy storage due to their high capacitance, fast charge–discharge rate and good cycling stability.[1,2] However, traditional supercapacitors are too bulky and heavy with specific capacities that are too low to be used in electric or hybrid vehicle applications as an auxiliary power source. To address this issue, significant effort has been devoted to the development of convenient, lightweight and stretchable ECs.[3–5] Recently, flexible fiber supercapacitors (FSCs) have emerged as ideal candidates for wearable energy storage devices. Wang and coworkers pioneered FSCs by growing ZnO nanotubes on two flexible polymer substrates (Kevlar fiber and poly(methyl methacrylate)) achieving a specific capacitance of 2.4 mF cm^{-2}.[6] Zou *et al.* adopted commercial pen ink as an active material for plastic-fiber based FSCs, and two parallel fibers were shown to give a specific capacitance of 11.9–19.5 mF cm^{-2}.[7] Peng and coworkers twisted aligned multi-walled carbon nanotube (CNT) fibers around Ti and Li wires in order to create micro-supercapacitors, which could function as solar energy storage devices with capacitance values of 0.6 mF cm^{-2} and 3.01 mF cm^{-2}, respectively.[8,9] Wei's and Miao's groups constructed double-ply yarn supercapacitors based on CNTs and polyaniline (PANI) nanowire arrays, which demonstrated capacitance values as high as 38 mF cm^{-2}.[10] Recently, Qu's group used glass pipe molds to fabricate all-graphene core–sheath fiber supercapacitors and these flexible supercapacitors exhibited capacitance values of 1.2–1.7 mF cm^{-2}.[11] However, the easy and scalable fabrication of flexible FSCs with a high capacitance and excellent cycling stability is still a big challenge that remains unresolved.

Carbon-based materials have earned a prominent reputation as ECs in the forms of 3D foams,[12–15] 2D plates[16–20] and 1D fibers,[21–23] because of their high specific surface areas, good stability, fine electrical conductivity and moderate costs.[2] As a newly discovered carbon allotrope with astonishing mechanical, thermal, and electrical attributes, graphene has been employed as a conductive matrix to make conventional plate ECs, generally by the addition/deposition of metal oxides (*e.g.*, MnO_2,[24–26] RuO_2[27] and ZnO[28,29]) or conductive polymers (*e.g.*, PANI[30–32] and polypyrrole[33,34]). Recently, continuous graphene fibers have been successfully fabricated through an industrially viable wet-spinning assembly approach, opening up an avenue towards wearable fiber-like graphene devices.[35–39]

Herein, for the first time, we explore the applications of graphene fiber supercapacitors (GFSs), made using a wet-spinning technology, which are continuous, mechanically strong, and favorably flexible. Due to the high specific surface area of the carbon based material and the uniform alignment of graphene sheets along the fiber axis, our GFSs demonstrated a high specific area capacitance (C_a) (3.3 mF cm^{-2} or 36.3 μF cm^{-1}, 3.77 F cm^{-3}), good flexibility (nearly 100% of the original state after 5000 bend cycles) and excellent electrochemical stability (nearly 100% of the original state after 5000 charge and discharge cycles). Given that the robust graphene fibers (GFs) are readily available on a large scale and the introduction of guest compounds (*e.g.*, metals, metal oxides and polymers) into the interspace between neighboring graphene sheets is easy to achieve, either by soaking or *in situ* deposition, the concept of GFSs should spark the rapid development of the next

[a]*MOE Key Laboratory of Macromolecular Synthesis and Functionalization, Department of Polymer Science and Engineering, Zhejiang University, 38 Zheda Road, Hangzhou 310027, P. R. China. E-mail: chaogao@zju.edu.cn*

[b]*National Center for Nanoscience and Technology, Beijing 100190, P. R. China. E-mail: weizx@nanoctr.cn*

† Electronic supplementary information (ESI) available. See DOI: 10.1039/c3ra44935a

generation of flexible electrical devices. Moreover, we have decorated polyaniline nanoparticles onto GFSs and the resulting pseudocapacitors demonstrated a capacitance of 66.6 mF cm^{-2} (731.9 μF cm^{-1} or 76.1 F cm^{-3}) at 0.1 mA cm^{-2}, a new record for fiber-shaped supercapacitors.

Results and discussion

GFs were made by wet-spinning aqueous graphene oxide (GO) liquid crystals into a coagulation bath of $CaCl_2$ aqueous–ethanol solution followed by chemical reduction *via* either hydrazine or hydroiodic acid, according to previously reported protocols,[36,40] and the resulting fibers are denoted as N_2H_4-GFs and HI-GFs, respectively. Good control over the diameter of GFs can be achieved using the spinning nozzle. The fibers can be continuously spun at room temperature to tens of meters long (or even thousands of meters if needed). The spinning process is very simple and green, and no toxic or corrosive solvents are used. Moreover, GO can be either bought commercially or readily produced on a large-scale by the oxidation of natural graphite. Hence, GFs are easily accessible for both newcomers and trained researchers. In comparison, continuous CNT fibers are much more difficult to obtain using either dry-spinning (which needs highly-aligned CNTs fabricated using precisely-controlled chemical-vapor deposition conditions in a high-temperature oven),[41] or wet-spinning (which normally requires the highly corrosive solvent chlorosulfonic acid and special apparatus to protect it from moisture) techniques.[42,43]

We fabricated GFS prototypes using the obtained reduced graphene fibers. Two GFs were fixed in parallel onto two electrodes between which an electrolyte was spread (Fig. 1a). Typically, the GFs used to make GFSs were ~3 cm in length and the effective part of each fiber immersed in the electrolyte was ~2 cm. The two similar GFs lie parallel to each other on a glass substrate and the distance between them is ~3 mm (Fig. 1b). In

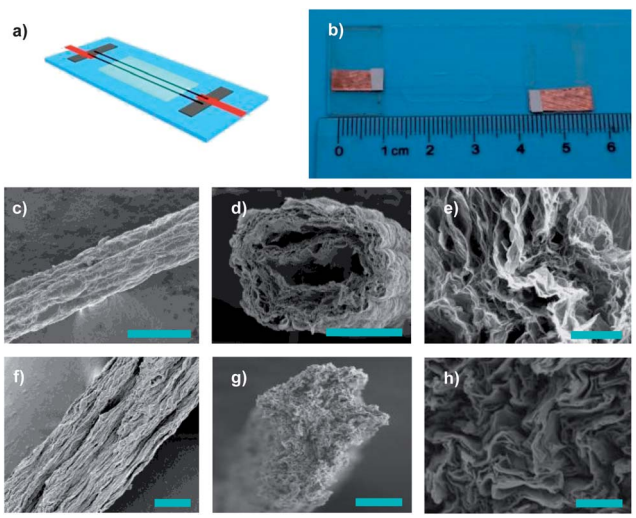

Fig. 1 (a) Schematic illustration of the graphene fiber supercapacitors (GFSs). (b) A photograph of a typical GFS device. (c–e) SEM images of N_2H_4-GFs. (f–h) SEM images of HI-GFs. Scale bars: (c) 100 μm, (d) 50 μm, (e) 10 μm, (f) 10 μm, (g) 10 μm, and (h) 1 μm.

previous reports,[6–9] fibers were twisted and integrated with each other in order to make a tight connection with the surface area or fixed parallel to each other using spacer wires. Here, we have made simpler supercapacitors with parallel fibers in order to demonstrate a model GFS and its potential. Liquid electrolytes such as H_2SO_4, Na_2SO_4, NaOH and other organic compounds are commonly used in traditional ECs.[2,44,45] In order to make stable and flexible devices, we chose PVA/H_3PO_4 gel with a low internal resistance as the electrolyte, which also separates the two fibers.[16]

Since different chemical reductions may result in different graphene structures, we selected two typical chemical reduction routes (*i.e.*, N_2H_4 and HI reduction) to make GFs and GFSs. Fig. 1c and f show the different microstructures of N_2H_4-GFs and HI-GFs. After chemical reduction, the widths of N_2H_4-GFs (~100 μm) are obviously bigger than those of HI-GFs (~35 μm). This is due to an expansion of GFs caused by gas generated during the N_2H_4 treatment, which has been previously observed in the N_2H_4 reduction of graphene-based bulk materials.[13] Looking at higher magnification images of the cross-sections of the fibers, N_2H_4-GFs appear to have widened towards the outside forming many holes (Fig. 1d), whereas HI-GFs are tighter with wrinkles all the way to the center (Fig. 1g).

The electrochemical performance of the GFSs was tested in a two-electrode system, which was believed to be a close approximation of a real capacitor. As shown in Fig. 2a and S1,† the cyclic voltammograms (CVs) of HI-GFS and N_2H_4-GFS are parallelogram shaped within the scan rate range of 10 to 100 mV s^{-1}. This indicates that the GFSs have the typical properties of carbon-based electrochemical double-layer capacitors.[46] The specific capacitance per gram was not believed to suitable in this case and C_a was preferred as a better means of evaluating the performance of the fiber shaped supercapacitors.[47] The C_a values of both HI-GFS and N_2H_4-GFS, based on the model of two face-to-face cylindrical electrodes, are shown in Table 1 (the calculation of C_a is described in ESI.†). We found that the C_a values of HI-GFS are 1.3 times higher than those of N_2H_4-GFS, according to the CV curves, which is in agreement with the results shown in the galvanostatic charge and discharge curves. The galvanostatic charge and discharge tests of GFSs were carried out at a current density of 0.1 mA cm^{-2} (Fig. 2b for HI-GFS and Fig. S2† for N_2H_4-GFS). Though N_2H_4-GFS demonstrated a C_a value as high as 2.5 mF cm^{-2} (78.5 μF cm^{-1} or 1.0 F cm^{-3}) at 0.1 mA cm^{-2}, according to the discharge curve, the curves are triangular shaped with high internal resistance (IR) drops (~0.18 V), which indicates that N_2H_4-GFS has a high internal resistance. Compared with N_2H_4-GFS, HI-GFS demonstrated a much higher C_a value (3.3 mF cm^{-2} or 36.3 μF cm^{-1} or 3.8 F cm^{-3}) and a much lower IR drop (~0.05 V) at a current density of 0.1 mA cm^{-2}. This phenomenon strongly suggested that HI-GFS performed much better than N_2H_4-GFS in their application as supercapacitors.

As for the reasons why GFSs obtained using different reducing methods demonstrate different electrochemical performance, we consider the most important one to be their different conductivities. It has been reported that the conductivity of a HI-reduced graphene film reached 29 800 S m^{-1},[48]

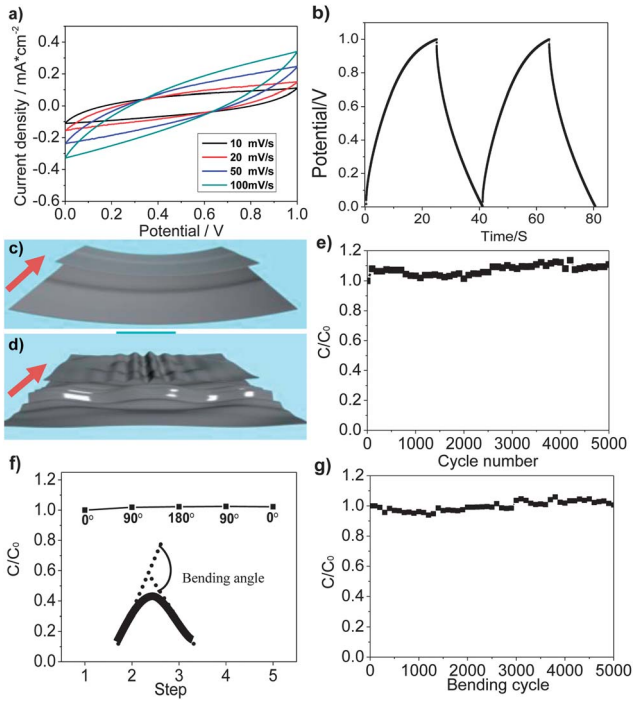

Fig. 2 Electrochemical analysis of GFSs. (a) CV curves of HI-GFS at scan rates of 100, 50, 20, and 10 mV s^{-1}, (b) galvanostatic charge and discharge curves of HI-GFS at a charge and discharge current density of 0.1 mA cm^{-2}. Schematic diagrams of the constituent graphene sheets in (c) N_2H_4-GFS and (d) HI-GFS indicate the flattened and wrinkled structures, which match the corresponding SEM inspections in Fig. 1e and h, respectively. The arrows in (c) and (d) indicate the fiber axis. (e) The charge–discharge cyclic stability of HI-GFS at a charge and discharge current density of 0.1 mA cm^{-2}. (f) Bending and relaxing stages for flexible PET membrane supported GFSs. (g) Capacitance retention as a function of cyclic bending number, showing the cyclic stability of HI-GFS under bending. C_0: the capacitance of the device for the galvanostatic charge and discharge curve of the first cycle at a current density of 0.1 mA cm^{-2}.

Table 1 C_a values of GFSs and GF-PANI at different scan rates based on the CV curves

Scan rate (mV s^{-1})	N_2H_4-GFS (mF cm^{-2})	HI-GFS (mF cm^{-2})	GF-PANI (mF cm^{-2})
100	1.4	1.8	3.8
50	2.5	2.7	10.0
20	4.4	5.1	20.7
10	7.3	9.4	35.4

which was much higher than that of a N_2H_4-reduced film (456 S m^{-1}).[40] In the case of our fibers, HI-GFs showed an electrical conductivity of ~10 000 S m^{-1}, which is an order of magnitude higher than that of N_2H_4-GFs (~700 S m^{-1}). The conductivity has a great influence on ECs. The different IR drops in the two systems also prove the importance of the electrical conductivity. Moreover, the inner micro-structures of GFs also play an important role in determining the properties of ECs. As can be seen from Fig. 1e, the N_2H_4-GFs contain many large pores (up to several μm), which are useless for the transportation of electrons, while the HI-GFs are relatively compact (Fig. 1h). The loose microstructures of N_2H_4-GFs, created by expansion during the reduction process, make the graphene sheets relatively flat (Fig. 2c), whereas the capillary reaction during the HI reduction leads to a plentiful amount of microscopic wrinkles in the graphene sheets in HI-GFs (Fig. 2d), which seems to be a structural factor that facilitates the improvement of C_a.[49]

Compared with previous reports, HI-GFS showed a relatively high capacitance. The C_a value (1.8 mF cm^{-2}) of our GFSs is almost 85% higher than that of previous graphene-based fiber supercapacitors prepared from graphene film using a scrolling process (0.97 mF cm^{-2}) at a scan rate of 100 mV s^{-1}.[21] Such a C_a value is slightly lower than that of other fiber supercapacitors (2.4 mF cm^{-2} at 100 mV s^{-1}),[6] but the GFSs are much more readily available.[36] In addition, the C_a value (3.3 mF cm^{-2}) calculated from the galvanostatic charge and discharge tests is much higher than the C_a value (<2.3 mF cm^{-2}) of pure CNT yarn-based supercapacitors at a current density of 0.1 mA cm^{-2}.[10] We also tested HI-GFS at a current density of 2.5 μA cm^{-1}, and it exhibited a C_a value of 1.1 mF cm^{-2} (or 12.1 μF cm^{-1}) (Fig. S3†), which is much higher than that of graphene-coated copper fiber supercapacitors (~0.73 mF cm^{-2} or 11.4 μF cm^{-1}).[22] In a previous report,[11] mold based all-graphene core–sheath fiber supercapacitors showed a C_a value 1.2–1.7 mF cm^{-2} (or 20 μF cm^{-1}) and such a capacitance is also lower than our spun graphene supercapacitors (3.3 mF cm^{-2} or 36.3 μF cm^{-1}) with compact structures. To the best of our knowledge, this is the highest C_a value ever reported for pure carbon-based fiber supercapacitors.

In order for GFSs to be suitable for real life use, we also tested the charge–discharge cyclic stability. According to Fig. 2e, no decrease of C_a was observed during the 5000 cycling tests at a charge–discharge current density of 0.1 mA cm^{-2}, demonstrating the excellent charge–discharge stability of HI-GFS. The flexibility of fiber-like ECs is also very important as they are usually under pressure when working. Neat GFs have exhibited good flexibility by forming tightened knots without breaking.[36] Accordingly, we also tested our GFSs using galvanostatic charge and discharge tests at different angles, in order to make sure that they have the potential to be practical in real life. In order to make a flexible device, we chose a flexible polyethylene terephthalate (PET) membrane to replace the glass substrate. Fig. 2f shows a constant capacitance retention for HI-GFS under different bending angles from 0 to 180° and back to 0°. Fig. S4† shows detailed photographs of the flexible GFSs at different bending angles. The capacitance retention was tested at 0.1 mA cm^{-2} and it shows that the capacitance experiences negligible fluctuation during the bending and relaxing processes. Moreover, the capacitance shows no decreasing trend even after 5000 bending cycles (Fig. 2g).

The superiority of the spinning assembly approach is reflected in the order of the graphene sheets in the bulk material, which results in a favourable fiber performance for supercapacitors. As mentioned above,[36] GFs were made from a pre-aligned liquid crystalline spinning dope, and the graphene sheets were further aligned into a more regular arrangement for the flow within the narrow spinning nozzle. Such a uniform orientation along the fiber axis enables the graphene fibers to be continuous, strong and flexible.

Furthermore, the continuous spinning protocol makes our wet-spinning graphene fibers available on a large scale. Accordingly, we fabricated long fiber-based GFSs up to tens of centimeters long. Fig. 3a shows four parallel fibers where each single fiber is as long as 20 cm. Fig. 3b and c show the bending state and the rolled state of the 20 cm long fibers fixed onto the PET membrane, respectively. Such supercapacitors are an order of magnitude longer than previous fiber ones. For the 20 cm long fiber supercapacitors, the parallel connecting circuit units were tested in order to probe their properties. Two units were connected in parallel and were measured in terms of CV at 100 mV s^{-1} (Fig. 3d). From the CV curves, the output current of the two parallel-connected units was increased by a factor of two at every moment compared with a single unit. This indicated that our fibers obey the theory of typical parallel capacitors. The total capacitance was ~1.7 mF with charge and discharge currents of 1 μA and a current density of 5 μA cm^{-2} (Fig. S5†).

Graphene has also been widely used as a conductive substrate for metal oxides and conductive polymers with pseudocapacitance that can greatly improve the properties of graphene-based supercapacitors.[50,51] Consequently, we used PANI as a model electroactive material in order to further improve the performance of our GFSs. The *in situ* PANI-doping process is described in the experimental section. Fig. 4a–c show the morphologies of the composites of HI-RGO and PANI at different magnifications. The PANI nanoparticles that were uniformly deposited onto the surface of the graphene fiber were 300–500 nm in diameter and 50–80 nm in height. Notably, the morphology of the PANI coated onto the HI-RGO fibers is different from a previous report, in which nanocones of PANI were formed using a dilute polymerization method. This is likely due to the reduced functional groups in the RGO fibers and the static nature of the reaction, which was conducted without stirring in our case.[10] The HI-RGO and PANI composite fibers can be easily packed into two parallel electrode supercapacitors (GF-PANI). This all-solid-state supercapacitor

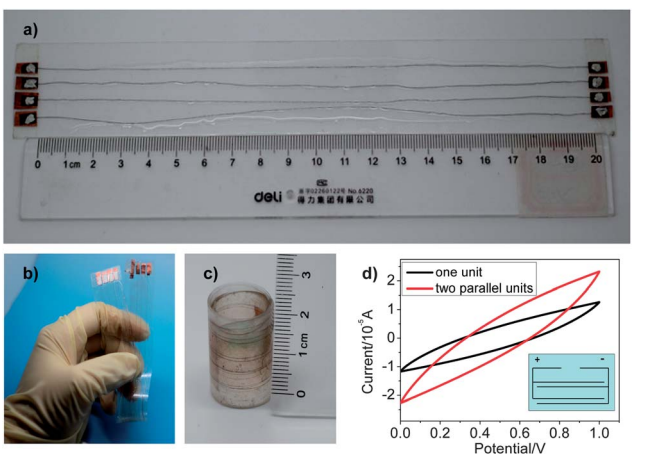

Fig. 3 Large-scale GFSs. Photographs of (a) the four parallel 20 cm long HI-GFs, (b) the bending state of the 20 cm long GFSs, and (c) the rolled state of the 20 cm long GFSs. (d) The CV curves for one single unit and two connected units of 20 cm long GFSs at a scan rate of 100 mV s^{-1}. The scheme in the inset of (d) shows the assembly of the two double-electrode GFSs.

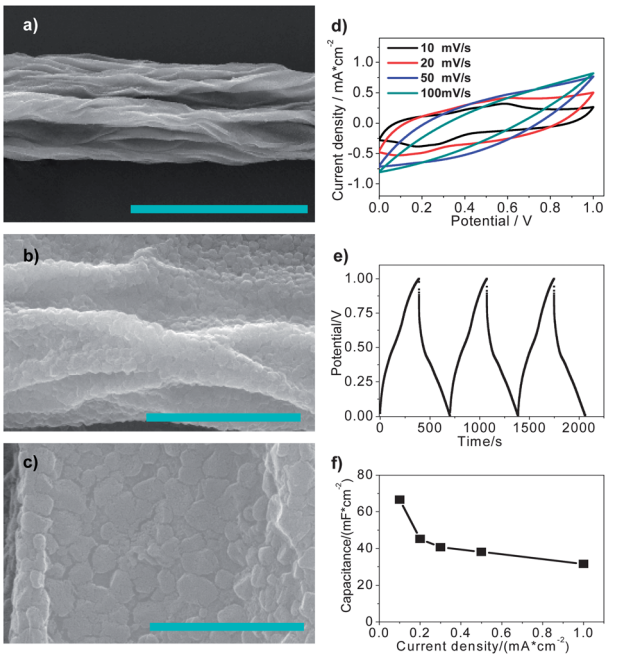

Fig. 4 (a–c) SEM images of GF-PANI. (d) The CV curves of GF-PANI at different scan rates varying from 10 to 100 mV s^{-1}. (e) Galvanostatic charge and discharge curves of GF-PANI at a current density of 0.1 mA cm^{-2}. (f) The value of C_a as a function of current density for GF-PANI. Scale bars: (a) 50 μm, (b) 5 μm, and (c) 2 μm.

retained the good physical characteristics of the graphene fiber, thus the flexible GF-PANI also exhibited an ultrahigh C_a value. Fig. 4d shows the CV curves of GF-PANI at different scan rates varying from 10 to 100 mV s^{-1}. The GF-PANI demonstrated two typical redox peaks, which are due to the pseudocapacitance of PANI at low scan rates, while the peaks became unclear at high scan rates. Such a phenomenon may be caused by the large distance (~3 mm) between the two electrodes, which results in a long time being needed for both charge and discharge. The C_a values of GF-PANI based on the CV curves are much larger than those of the pure graphene fibers (Table 1).

Fig. 4e shows the galvanostatic charge and discharge curves of GF-PANI at a current density of 0.1 mA cm^{-2}. The charge and discharge lines are not smooth like HI-GFS. The discharge curve of GF-PANI exhibited two voltage stages: a stage between 1.0–0.45 V of double-layer capacitance with a short time duration and a stage between 0.45–0 V of both double-layer capacitance and pseudocapacitance.[32] According to the discharge curve, GF-PANI demonstrates an ultrahigh C_a of 66.6 mF cm^{-2} (731.9 μF cm^{-1} or 76.1 F cm^{-3}) at a current density of 0.1 mA cm^{-2}, which is 20 times higher than the pure HI-GFS. Fig. 4f shows the relationship between the current density and C_a of GF-PANI. C_a decreased from 66.6 to 31.5 mF cm^{-2} as the current density increased from 0.1 to 1.0 mA cm^{-2}. The C_a value of our fibers (31.5 mF cm^{-2}) was 2.6 times larger than that of a two-ply yarn supercapacitor made of CNTs and PANI (12 mF cm^{-2}) due to their high surface area for the deposition of PANI.[10] This indicates that our GFs are a superior supercapacitor substrate for conductive polymers, which can greatly improve the supercapacitor performance of devices.

Experimental and characterization

Preparation of GFSs

GO fibers were prepared according to the protocol described previously,[36] using a coagulation bath of 5 wt% $CaCl_2$ aqueous–ethanol solution (3 : 1 by volume). The chemically converted graphene fibers were prepared either by immersing them in hydroiodic acid (30%) at 80 °C for 8 h (HI-GFs) or bathing them in hydrazine vapor in a sealed vessel containing hydrazine hydrate at 80 °C for 8 h (N_2H_4-GFs). Two GFs were fixed onto a substrate in parallel, and then covered with the PVA–H_3PO_4–H_2O (1 : 1 : 10 by mass) gel electrolyte, affording a GFS (Fig. 1a and b).

Preparation of GF-PANI

0.116 g aniline was dropped into a bottle, which contained 5 mL ethanol and 15 mL 1 M perchloric acid. This was stirred for half an hour before a GF was immersed into the mixture. Afterwards, the mixture was left to stand for 1 hour before the dropwise addition of 0.19 g ammonium persulfate in 5 mL perchloric acid. The reaction was kept at −10 °C without stirring for 24 hours. The resulting GF-PANI was then washed with 0.1 M perchloric acid, dried under vacuum and assembled into a GF-PANI supercapacitor following the same procedure as the preparation of GFSs.

Characterization

Cyclic voltammetry and galvanostatic charge and discharge measurements were performed using an electrochemical workstation (CHI660e, CH Instruments, Inc.). The morphologies of the fibers were characterized with scanning electron microscopy (SEM) (Hitachi S3000N).

Conclusions

In summary, we have successfully made the first prototypes of neat wet-spun graphene fiber supercapacitors. Such supercapacitors demonstrated good electrochemical properties with excellent flexibility and cycling stability. The performance of the graphene fiber supercapacitors can be greatly improved by introducing other capacitive materials such as conducting PANI. The graphene fiber supercapacitors integrate the merits of the cost-effective graphite raw material, large-scale availability of chemically converted graphene, good flexibility, unique attributes of graphene, and a simple and green fabrication process, breaking new ground in the development of flexible/wearable electrical devices.

Notes and references

1 J. R. Miller and P. Simon, *Science*, 2008, **321**, 651.
2 P. Simon and Y. Gogotsi, *Nat. Mater.*, 2008, **7**, 845.
3 D. Pech, M. Brunet, H. Durou, P. Huang, V. Mochalin, Y. Gogotsi, P. Taberna and P. Simon, *Nat. Nanotechnol.*, 2010, **5**, 651.
4 C. J. Yu, C. Masarapu, J. P. Rong, B. Q. Wei and H. Q. Jiang, *Adv. Mater.*, 2009, **21**, 4793.
5 L. B. Hu, M. Pasta, F. La Mantia, L. F. Cui, S. Jeong, H. D. Deshazer, J. W. Choi, S. M. Han and Y. Cui, *Nano Lett.*, 2010, **10**, 708.
6 J. Bae, M. K. Song, Y. J. Park, J. M. Kim, M. L. Liu and Z. L. Wang, *Angew. Chem., Int. Ed.*, 2011, **50**, 1683.
7 Y. P. Fu, X. Cai, H. W. Wu, Z. B. Lv, S. C. Hou, M. Peng, X. Yu and D. C. Zou, *Adv. Mater.*, 2012, **42**, 5713.
8 T. Chen, L. B. Qiu, Z. B. Yang, Z. B. Cai, J. Ren, H. P. Li, H. J. Lin, X. M. Sun and H. S. Peng, *Angew. Chem., Int. Ed.*, 2012, **51**, 11977.
9 J. Ren, L. Li, C. Chen, X. L. Chen, Z. B. Cai, L. B. Qiu, Y. G. Wang, X. R. Zhu and H. S. Peng, *Adv. Mater.*, 2013, **25**, 1155.
10 K. Wang, Q. H. Meng, Y. J. Zhang, Z. X. Wei and M. H. Miao, *Adv. Mater.*, 2013, **25**, 1494.
11 Y. N. Meng, Y. Zhao, C. G. Hu, H. H. Cheng, Y. Hu, Z. P. Zhang, G. Q. Shi and L. T. Qu, *Adv. Mater.*, 2013, **25**, 2326.
12 X. H. Cao, Y. M. Shi, W. H. Shi, G. Lu, X. Huang, Q. Y. Yan, Q. C. Zhang and H. Zhang, *Small*, 2011, **7**, 3163.
13 Z. Q. Niu, J. Chen, H. H. Hng, J. Ma and X. D. Chen, *Adv. Mater.*, 2012, **24**, 4144.
14 Y. Zhao, C. G. Hu, Y. Hu, H. H. Cheng, G. Q. Shi and L. T. Qu, *Angew. Chem., Int. Ed.*, 2012, **51**, 11174.
15 Z. S. Wu, Y. Sun, Y. Z. Tan, S. B. Yang, X. L. Feng and K. Müllen, *J. Am. Chem. Soc.*, 2012, **134**, 19532.
16 M. Kaempgen, C. K. Chan, J. Ma, Y. Cui and G. Gruner, *Nano Lett.*, 2009, **9**, 1872.
17 C. Meng, C. Liu, L. Chen, C. Hu and S. Fan, *Nano Lett.*, 2010, **10**, 4025.
18 K. H. An, W. S. Kim, Y. S. Park, Y. C. Choi, S. M. Lee, D. C. Chung, D. J. Bae, S. C. Lim and Y. H. Lee, *Adv. Mater.*, 2001, **13**, 497.
19 L. B. Hu, J. W. Choi, Y. Yang, S. Jeong, F. La Mantia, L. F. Cui and Y. Cui, *Proc. Natl. Acad. Sci. U. S. A.*, 2009, **106**, 21490.
20 H. M. Jeong, J. W. Lee, W. H. Shin, Y. J. Choi, H. J. Shin, J. K. Kang and J. W. Choi, *Nano Lett.*, 2011, **11**, 2472.
21 X. M. Li, T. S. Zhao, K. L. Wang, Y. Yang, J. Q. Wei, F. Y. Kang, D. H. Wu and H. W. Zhu, *Langmuir*, 2011, **27**, 12164.
22 Y. Li, K. X. Sheng, W. J. Yuan and G. Q. Shi, *Chem. Commun.*, 2013, **49**, 291.
23 J. A. Lee, M. K. Shin, S. H. Kim, H. U. Cho, G. M. Spinks, G. G. Wallace, M. D. Lima, X. Lepro, M. E. Kozlov, R. H. Baughman and S. J. Kim, *Nat. Commun.*, 2013, **4**, 1970.
24 G. H. Yu, L. B. Hu, N. A. Liu, H. L. Wang, M. Vosgueritchian, Y. Yang, Y. Cui and Z. N. Bao, *Nano Lett.*, 2011, **11**, 4438.
25 Q. Cheng, J. Tang, J. Ma, H. Zhang, N. Shinya and L. C. Qin, *Carbon*, 2011, **49**, 2917.
26 S. Chen, J. W. Zhu, X. D. Wu, Q. F. Han and X. Wang, *ACS Nano*, 2010, **4**, 2822.
27 Z. S. Wu, D. W. Wang, W. Ren, J. Zhao, G. Zhou, F. Li and H. M. Cheng, *Adv. Funct. Mater.*, 2010, **20**, 3595.
28 Y. L. Chen, Z. A. Hu, Y. Q. Chang, H. W. Wang, Z. Y. Zhang, Y. Y. Yang and H. Y. Wu, *J. Phys. Chem. C*, 2011, **115**, 2563.
29 X. C. Dong, Y. F. Cao, J. Wang, M. B. Chan-Park, L. H. Wang, W. Huang and P. Chen, *RSC Adv.*, 2012, **2**, 4364.
30 J. J. Xu, K. Wang, S. Z. Zu, B. H. Han and Z. X. Wei, *ACS Nano*, 2010, **4**, 5019.

31 K. Zhang, L. L. Zhang, X. S. Zhao and J. S. Wu, *Chem. Mater.*, 2010, **22**, 1392.
32 Q. Wu, Y. X. Xu, Z. Y. Yao, A. R. Liu and G. Q. Shi, *ACS Nano*, 2010, **4**, 1963.
33 S. Biswas and L. T. Drzal, *Chem. Mater.*, 2010, **22**, 5667.
34 P. A. Mini, A. Balakrishnan, S. V. Nair and K. R. V. Subramanian, *Chem. Commun.*, 2011, **47**, 5753.
35 Z. Xu and C. Gao, *ACS Nano*, 2011, **5**, 2908.
36 Z. Xu and C. Gao, *Nat. Commun.*, 2011, **2**, 571.
37 Z. Xu, H. Y. Sun, X. L. Zhao and C. Gao, *Adv. Mater.*, 2013, **25**, 188.
38 Z. Xu, Y. Zhang, P. G. Li and C. Gao, *ACS Nano*, 2012, **6**, 7103.
39 X. Z. Hu, Z. Xu and C. Gao, *Sci. Rep.*, 2012, **2**, 767.
40 I. K. Moon, J. Lee, R. S. Ruoff and H. Lee, *Nat. Commun.*, 2010, **1**, 73.
41 M. Zhang, K. R. Atkinson and R. H. Baughman, *Science*, 2004, **306**, 1358.
42 N. Behabtu, C. C. Young, D. E. Tsentalovich, O. Kleinerman, X. Wang, A. W. K. Ma, E. A. Bengio, R. F. ter Waarbeek, J. J. de Jong, R. E. Hoogerwerf, S. B. Fairchild, J. B. Ferguson, B. Maruyama, J. Kono, Y. Talmon, Y. Cohen, M. J. Otto and M. Pasquali, *Science*, 2013, **339**, 182.
43 N. Behabtua, M. J. Greena and M. Pasquali, *Nano Today*, 2008, **3**, 24.
44 A. G. Pandolfo and A. F. Hollenkamp, *J. Power Sources*, 2006, **157**, 11.
45 M. D. Stoller, S. J. Park, Y. W. Zhu, J. H. An and R. S. Ruoff, *Nano Lett.*, 2008, **8**, 3498.
46 E. Frackowiak and F. Beguin, *Carbon*, 2001, **39**, 937.
47 Y. Gogotsi and P. Simon, *Science*, 2011, **334**, 917.
48 S. F. Pei, J. P. Zhao, J. H. Du, W. C. Ren and H. M. Cheng, *Carbon*, 2010, **48**, 4466.
49 Y. W. Zhu, S. Murali, M. D. Stoller, K. J. Ganesh, W. W. Cai, P. J. Ferreira, A. Pirkle, R. M. Wallace, K. A. Cychosz, M. Thommes, D. Su, E. A. Stach and R. S. Ruoff, *Science*, 2011, **332**, 1537.
50 X. Huang, Z. Y. Zeng, Z. X. Fan, J. Q. Liu and H. Zhang, *Adv. Mater.*, 2012, **24**, 5979.
51 Y. Huang, J. J. Liang and Y. S. Chen, *Small*, 2012, **8**, 1805.

